

# On The Inelastic Behavior of Shield Tunnels in Kobe City During Hyogo-Ken Nanbu Earthquake

Shiro Takada<sup>1)</sup> and Mostafa Abd El-Aziz<sup>2)</sup>

1) Professor, Department of Civil Engineering, Kobe University, 1-1 Rokkodai, Nada, Kobe 657

2) Ph.D. Student, Graduate School of Science & Technology, Kobe University, 1-1 Rokkodai, Nada, Kobe 657

Based on the seismic deformation method, a new finite element inelastic model is developed to analyze the transverse direction of shield tunnels. The model is subjected to ground displacements and shear stresses determined from the free field earthquake response. The response is determined by applying increments of the external forces. The incremental and the total forces (stresses) in the tunnel (ground springs) are determined. The updated coordinates and stiffness matrices can be determined according to the new elastic/inelastic conditions. The model is utilized in studying the response of sewage shield tunnels at Takamatsu (with secondary lining) and at Karimojima (without secondary lining) in Kobe City during Hyogo-Ken Nanbu Earthquake.

**Key Words :** Finite elements, inelastic analysis, seismic deformation method, soil-structure interaction, shield tunnels, segment joints, secondary lining

## 1. Introduction

Hyogo-Ken Nanbu Earthquake of January 17th 1995 caused some damage to several small and medium-diameter shield tunnels. Some of those tunnels were unfunctional for a period of time due to the leakage of ground water inside the tunnels through cracks developed by the earthquake. The purpose of this research is to study the inelastic behavior of the transverse direction of shield tunnels under high level ground motions. A new inelastic ground-tunnel model is proposed and utilized in studying the inelastic response and damage of sewage shield tunnels at Takamatsu (with secondary lining) and at Karimojima (without secondary lining) in Kobe City during Hyogo-Ken Nanbu Earthquake.

## 2. Analytical Model of Ground-Tunnel System

The proposed tunnel-ground system illustrated in Fig.1 is composed of: (1) Curved beam elements representing the tunnel segments and secondary lining with a trilinear moment-curvature relationship to account for concrete cracking, reinforcing steel yielding, and concrete crushing. The idealized stress-strain relationships of concrete and steel are based on the Japanese Standard Specification<sup>(1)</sup>. The interaction between axial force and bending moment in developing concrete cracks, reinforcing steel yield, and concrete crush is ignored because the stresses due to bending moment is dominant in the total seismic stress. (2) Joint elements representing the composite connection of the segment joints with the secondary lining. (3) Ground springs representing soil-structure interaction, in which sliding and separation are taken into account. The base rock is specified by the design guidelines<sup>(2)</sup> as that layer whose shear wave velocity exceeds 300m/sec. Seismic forces due to ground displacements are applied to the system through the end of the interaction spring, while those due

to ground shear stresses are applied directly on the tunnel nodes.

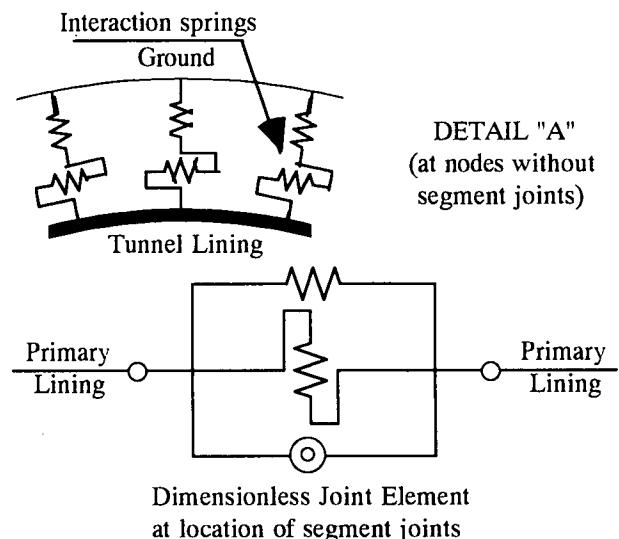
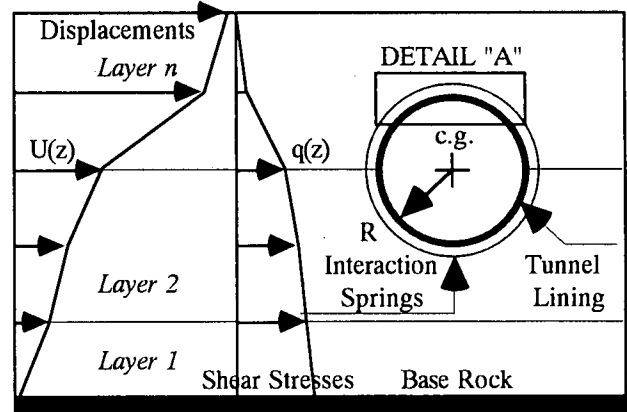


Fig.1 Tunnel-Ground system

### 3. Inelastic Model of Segment Joints

A typical connection at the location of segment joints is sketched in Fig.2 for tunnels without secondary lining. The compatibility of deformations of the joint implies:

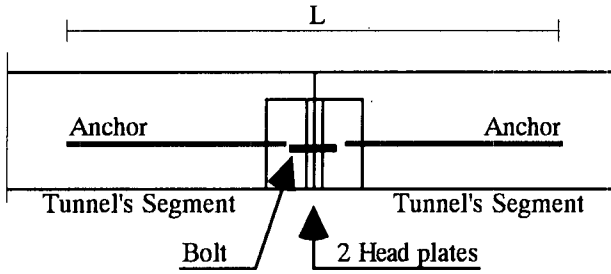


Fig.2 Typical Connection at segment joint

$$\Delta_{EQ} = 2 \Delta_P + \Delta_B \quad (1)$$

in which  $\Delta_{EQ}$ ,  $\Delta_P$  and  $\Delta_B$  are the deformations of the equivalent connection, head plate, and segment bolt. Then the tensile stiffness is determined from:

$$K_{EQ} = K_B K_P / (2K_B + K_P) \quad (2)$$

in which  $K_{EQ}$ ,  $K_P$  and  $K_B$  are the stiffnesses of the equivalent connection, head plate, and segment bolt.  $K_P$ ,  $K_B$  are already derived in the literature<sup>(3)</sup>. Fig.3 shows the calculation model for determining the flexural stiffness of the segment joint, which can be determined by applying the equations of compatibility and equilibrium of forces.

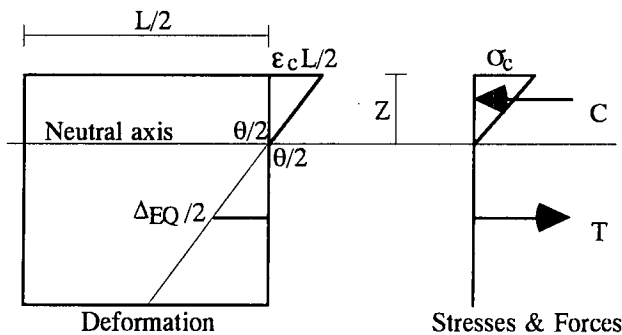


Fig. 3 Model for determining the flexural stiffness

### 4. Numerical Analyses

A study on the inelastic response of two shield tunnels serving the sewage system of Kobe City during Hyogo-Ken Nanbu earthquake is performed. One tunnel of 2.00m diameter without secondary lining is located at Karimojima (at level 51.4m), while the other of 3.40m diameter with secondary lining is located at Takamatsu (at level 57m). The trilinear moment-curvature relationships and the cross section dimensions and reinforcement of the tunnels are shown in Fig.4, while the inelastic behavior of their segment joints are shown in Figs.5&6. The accelerograms of Port Island at -83m of ground surface (of maximum horizontal and vertical accelerations of 679 & 187 cm/sec<sup>2</sup>) are used in the FEM free field analysis of the ground conditions shown in Fig.7.

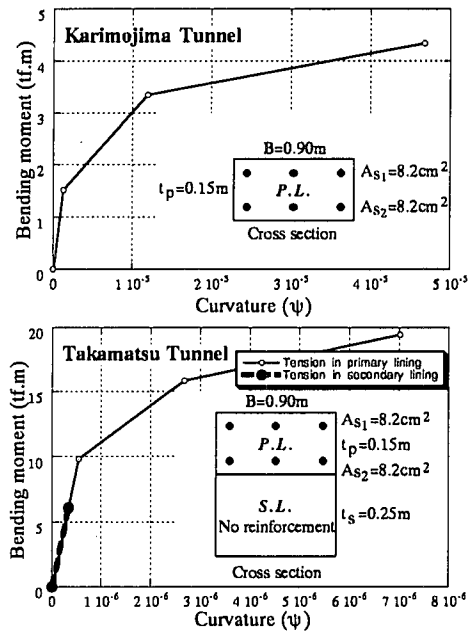


Fig.4 Trilinear moment-curvature relationships

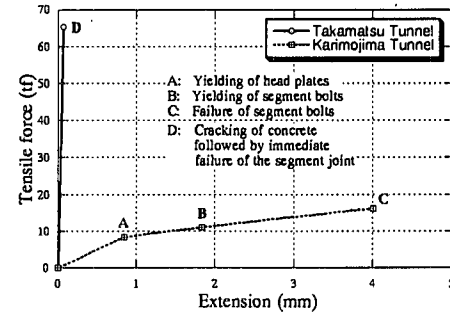


Fig.5 Inelastic behavior of segment joints in tension

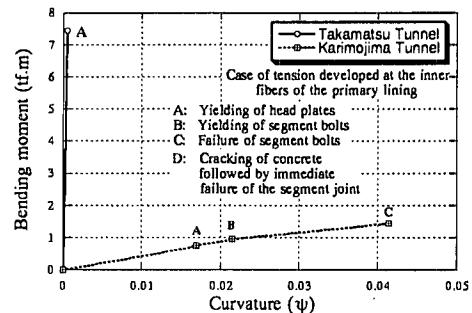


Fig.6 Inelastic behavior of segment joints in flexure

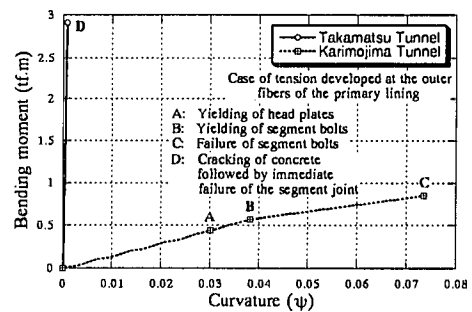


Fig.6 Inelastic behavior of segment joints in flexure

### 5. Discussion of Results

The maximum ground displacements of the FEM free field analysis are shown in Fig.8. The bottom stiff layers

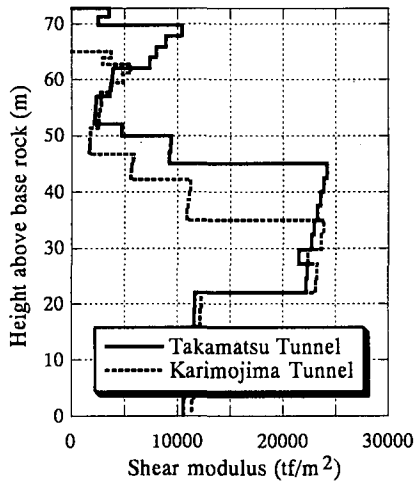


Fig.7 Shear rigidity of various ground layers

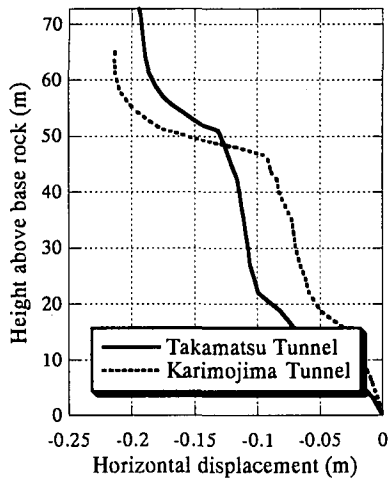


Fig.8 Maximum ground displacements

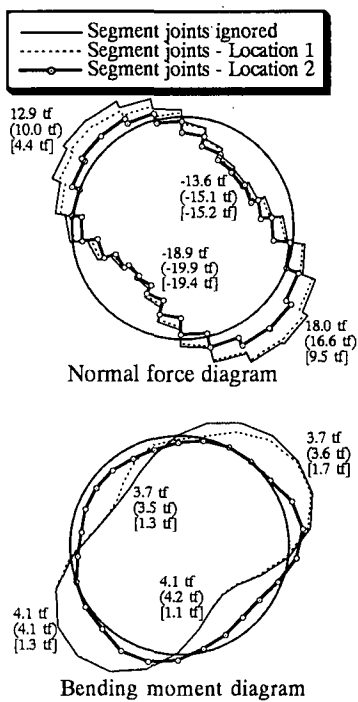


Fig.9 Response of Karimojima tunnel

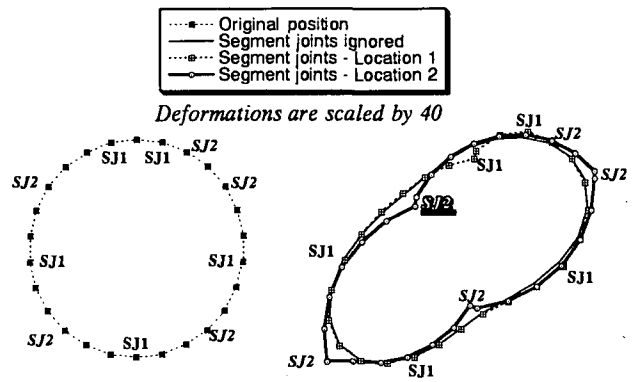


Fig.10 Deformation of Karimojima tunnel

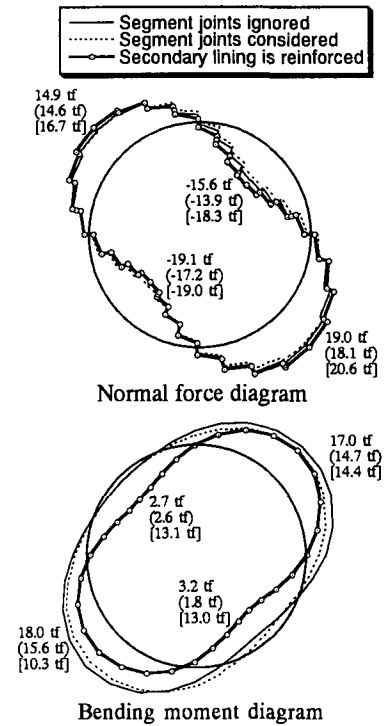


Fig.11 Response of Takamatsu tunnel

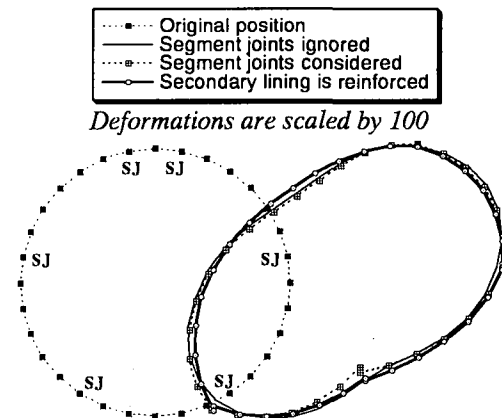


Fig.12 Deformation of Takamatsu tunnel

show remarkable deformations although their shear wave velocities exceed 300m/sec. The reason for such ground behavior is that the rigidity of the lowest layer is about half that of the layer above.

#### Response of Karimojima Tunnel

Figs.9&10 show the internal force diagrams and deformations of Karimojima tunnel. Three cases are considered. In the first case, the influence of segment joints is ignored, while is considered in the second case as shown in Fig.10 denoted by SJ1. Although the tensile and the flexural stiffnesses of segment joints are much less than those of the tunnel, the general response is almost the same. This is because the segment joints are located very near to the position of zero normal forces and bending moments. However, their influence is remarkable in redistributing the axial forces in the tunnel, in which tensile forces are significantly reduced while compression forces are slightly increased. Moreover, bending moments are slightly redistributed at the portion around the two top segment joints, where a different deformation pattern is also remarkable. The maximum deformations of segment joints are 0.27mm & 0.75mm due to tension and bending moment, from which 0.18mm is a plastic deformation. Concrete crack and steel yield at 12% & 43% of the total seismic forces, while the head plates of segment joints yield at 73%. Moreover, half of contact nodes slide at 8% while separation start at 71%. At the end of the analysis, 94% & 10% of the contact nodes slid and separated.

Since the rings of shield tunnels are constructed in a staggered sense, a third case is considered in which the position of the segment joints is shown in Fig.10 denoted by SJ2. In this case, the tensile forces and the bending moments are highly reduced. This is because the segment joints are located near to the position of maximum normal forces and bending moments, which are reduced in order to match with the small stiffnesses and strengths of segment joints. On the other hand, the deformations are increased as shown in Fig.10. The maximum deformations of segment joints are 0.83mm & 2.02mm due to tension and bending moment, from which 2.01mm is a plastic deformation. Concrete crack at 89% of the total applied seismic forces, while the head plates and bolt of segment joints yield at 36% & 73%. Moreover, half of contact nodes slide at 10%, while separation started at 50%. At the end of the analysis, 94% & 29% of the contact nodes slid and separated. The second case is critical for the primary lining, while the third case is critical for the segment joints.

#### Response of Takamatsu Tunnel

Figs.11&12 show the internal force diagrams and deformations of Takamatsu tunnel. Three cases are considered. In the first case, the influence of segment joints is ignored, while is considered in the second case as shown in Fig.12. The secondary lining is not reinforced (old tunnel), which is currently not recommended, as verified by its brittle behavior in Figs.4,5&6. Therefore, minimum reinforcement is considered in the third case. The reinforcement is determined based on the difference in the strength of the primary lining and the segment joint. The influence of segment joints and reinforcement of the

secondary lining is remarkable in redistributing the axial forces and bending moments in the tunnel. In the first two cases, bending moments developing tension inside the tunnel are much less than those developing tension outside the tunnel because the utilized corresponding flexural stiffnesses are quite different. However, the maximum values of these moments become close to each in the third case, because the utilized corresponding stiffnesses are close. Moreover, the deformations of the three cases are almost identical. For the second case, concrete crack at 23% of the total seismic forces, while half of contact nodes slide at 31% and separation did not occur. At the end of the analysis, 95% of the contact nodes slid. For the third case, concrete crack and steel yield at 20% & 85% of the total applied seismic forces, while the head plates of segment joints yield at 45%. On the other hand, half of contact nodes slide at 11%, and separation did not occur. At the end of the analysis, 95% of the contact nodes slid.

#### 6. Conclusions

Within the numerical results of the cases studied and discussions, the main conclusions are:

1. A realistic assumption for the location of the stiff layer that represents the base rock is necessary for the seismic analysis. This layer shall not be followed by a weaker one.
2. The inelastic behavior of the interaction springs is mainly due to sliding of most of the contact nodes, while separation is very limited.
3. The inelastic behavior of the analyzed tunnels, is mainly due to concrete cracking developed at low levels of seismic forces, then yield of segment joints and reinforcing steel developed at moderate and high levels of seismic forces.
4. Segment joints redistribute and may reduce the internal forces in the tunnel. However, for shield tunnels without secondary lining, the deformation of segment joints is very high and may exceed the elastic range leading to leakage of ground water inside the tunnel.
5. It seems that the choice of Port Island acceleration records as input for the free field analysis was not appropriate and do not represent the actual accelerations that occurred at the site during Hyogo-Ken Nanbu earthquake, because no cracks were reported for the tunnel.

#### References

- 1) Japanese Standard Specification for Design and Construction of Concrete Structures, Part (Design), 1986 Edition, English Version.
- 2) H. Asakura, K. Kawashima, and H. Sugita: Guidelines for Seismic Design Methods of Large Underground Structures. 24th Joint Meeting of the U.S. - Japan Cooperative Program in Natural Resources, Panel on Wind and Seismic Effects, Gaithersburg, MD, U.S.A., pp. 39-53, May 1992.
- 3) K. Kawashima, H. Sugita, T. Kanoh, N. Obinata, and Y. Shiba: Seismic Design Method of Reinforced Concrete Shield Tunnels. Report of Public Work Research Institute, Ministry of Construction, Vol. 188, March 1993. (*in Japanese*)